A robust optimization model for prosumer microgrids considering uncertainties in prosumer generation

Uyikumhe Damisa[1], Nnamdi I. Nwulu[1*], Yanxia Sun[1]

[1]Department of Electrical and Electronic Engineering Science, University of Johannesburg, Corner Kingsway and University Road, Auckland, Johannesburg, South Africa.

[*]nnwulu@uj.ac.za

1 Abstract

Recent times have seen the emergence of prosumers with undispatchable renewable onsite generators, which can complicate operational planning of grids. The complication can be exacerbated when prosumers have the leeway to export excess generation to the grid, which may necessitate the development of a new paradigm for the operational planning of prosumer grids. In this paper, a computationally tractable robust microgrid operational dispatch model which uses diesel generators, a battery and interruptible loads to handle uncertainty in prosumer generation is proposed. Using the modified version of a microgrid in Guangdong Province, China, the CPLEX solver in the Advanced Interactive Multidimensional Modelling System environment is used to validate the effectiveness of the proposed model. The proposed robust model yields a higher objective function value than its deterministic counterpart; however, it guarantees system reliability under any realization of prosumer generation within specified bounds, which the deterministic model cannot guarantee. Further analysis shows that the optimal objective function value increases with the uncertainty level of prosumer generation.

2 Nomenclature

2.1 Sets

g, G	Diesel generator index, number of diesel generators
p, P	Prosumer index, number of prosumers

2.2 Parameters

Δt	Interval size
a_g, b_g	Cost coefficients of diesel generator g [\$/(MW^{2}h)]/ [\$/MWh]

c_g	Reserve cost factor for diesel generator g
d_g	Cost per unit of up & down regulation of diesel generator g [$/MW]
e	Cost per unit of load curtailed [$/MW]
f	Battery charging/discharging cost factor [$/MW^2]
P_g^{min} & P_g^{max}	Minimum and maximum output limits of diesel generator g [MW]
R_g^U & R_g^D	Maximum up & down regulation of diesel generator g [MW]
Res	Reserve requirement [MW]
$UReg$ & $DReg$	Required up & down regulation reserve [MW]
P_g^{curr}	Current output of diesel generator g [MW]
P_{curt}^{max}	Available load curtailment capacity [MW]
P_{bToFro}^{max}	Maximum power transfer to/from battery [MW]
E_b	Current battery content [MWh]
E_b^{min}& E_b^{max}	Minimum & maximum battery content [MWh]
$P_{proGen,p}^{FC}$	Power output forecast of prosumer p's generator [MW]
$P_{proDem,p}$	Prosumer p's demand [MW]
P_D	Grid demand (excluding prosumer demand) [MW]

2.3 Variables

P_g^{sch}	Scheduled output of diesel generator g [MW]
P_g^{res}	Scheduled reserve from diesel generator g [MW]
P_g^{UReg}	Scheduled up regulation reserve from diesel generator g [MW]
P_g^{DReg}	Scheduled down regulation reserve from diesel generator g [MW]
P_{curt}^{sch}	Scheduled load curtailment [MW]
P_{bToFro}^{sch}	Scheduled power transfer to/from battery [MW]
$P_{ToFroPro,p}$	Power transfer to/fro prosumer p [MW]

3 Introduction

Due to declining costs of solar energy systems and growing concerns over environmental pollution, among other factors, recent times have seen an emergence of a new kind of electricity consumers known as prosumers. Prosumers differ from consumers in that they own onsite generating facilities and can export electricity to the grid or other consumers [1]. While some prosumers' local generators are dispatchable, most are undispatchable. Operators of grids (microgrid operators (MGO's) for microgrids (MG's)) that interconnect prosumers with undispatchable generation, especially if prosumers possess the license to export unused, surplus energy to the grid, are faced with an increased level of grid power supply/demand uncertainty. Hence, operational planning in prosumer grids could be more challenging. A promising approach to uncertainty handling in prosumer power grids is the involvement of demand-side resources in the operational planning of these grids.

The involvement of demand-side resources in grid operations continues to attract the attention of researchers. The authors of [2] proposed a market model for the joint dispatch of energy and reserve in which electricity generators and consumers can both bid for energy and a number of reserve products. They reported that considerable social welfare gains may be derived from the additional scheduling flexibility that the provision of reserve capacities by demand-side resources provides. In [3], a study was carried out on a renewable energy-assisted MG which interconnects both commercial and industrial loads. Using various demand response programs, loads were involved in the energy and reserve dispatch process, and as a result, the MG's operating cost dropped. A similar observation was made in [4] where a stochastic energy and reserve dispatch optimization model was proposed. In the paper, uncertainty in renewable generation was handled using reserve capacities from loads and diesel generators (DG's); and with the participation of these demand-side resources, DG usage reduced as well as grid operating cost. Demand-side participation in energy and reserve dispatch was also studied on a smart distribution grid in [5]. In the paper, demand response aggregators aggregated load reduction offers from small and medium scale customers. Results obtained from investigating a distribution system corroborate those in [4] and [3]. The authors of [6] proposed an energy and reserve dispatch model for an MG with RE sources. In their proposed model, uncertainty in wind and solar power was balanced using demand-side resources, dispatchable generators and energy from the main grid. Aggregation of the behind-the-meter resources of large prosumers for participation in the energy and reserve dispatch process of a renewable energy - assisted MG was proposed in [7]. The prosumer's resources considered were flexible loads and batteries, and the MG's operating cost was seen to reduce with their involvement. In [7], however, uncertainties in RE generation and load were not taken into account.

The literature is replete with various approaches to operational planning in MG's. One widely studied approach is the scenario-based method of handling uncertainties in operational dispatch models. A mixed-integer, non-linear energy and reserve dispatch formulation for an MG was developed in [8]. Wind speed and load were modelled using appropriate probability distribution functions, and different scenarios were generated using segmented probability distribution functions. MG operating cost and emission were minimized using the multi-objective formulation proposed in [9]. Various scenarios were generated using discretized probability distribution functions for solar irradiation, wind speed and load, but only the most likely scenarios were utilized in the formulation. With the aim of minimizing both operating and investment costs of an MG, a two-stage stochastic formulation was proposed in [10]. The scenario tree approach was used to model fluctuations in wind, solar and demand. In [11], uncertainties in solar, wind, load and price of electricity were handled in a proposed scenario-based approach. Forecasts were generated, and then multiple scenarios were constructed using the Monte Carlo Simulation with Latin Hypercube Sampling method. A scenario reduction approach was further applied to reduce computational time. The Monte Carlo Simulation is known to be a reasonably precise method of handling uncertainties; however computational burden can be very high for a large number of scenarios [8]. Moreover, it can be challenging to obtain accurate probability distribution functions for real life applications [12].

Another technique for solving optimization problems with uncertain parameters is the chance-constrained technique. It was used in [13] for a grid-connected MG, to handle demand and renewable energy (RE) uncertainties. A shortcoming of the technique is that the resulting model can be difficult to solve [14]. They are also usually intractable [15].

In the literature, robust optimization models have also been used to handle uncertainties in model parameters. In [16], load and RE uncertainty were modelled by an uncertainty set, and a scenario-based robust optimization model was used to generate an optimal solution that is robust against most of the possible realizations of demand and RE supply within the uncertainty set. The long term average operating cost of a grid was minimized with the use of a robust optimization technique in [17]. In the paper, the technique was used to handle worst-case realizations of load and RE generation modelled by bounded uncertainty sets. A two-stage robust optimization model was proposed in [18] to minimize MG operating cost under worst-case realization of grid connection status and RE generation. In [19], a robust energy dispatch model was proposed to generate an optimal solution that is robust against any realization of uncertain parameters. Also, a robust approach to energy and ancillary services co-optimization in real-time markets was presented in [12]. In the paper, the approach generated optimal generator base points that are robust against any realization of uncertainty within a bounded uncertainty set. A robust approach to energy dispatch optimization in a renewable energy-assisted prosumer MG with demand response aggregators was presented in [20]. The ability to produce reasonable results even if realization of uncertainty is outside the forecasted uncertainty set is one strength of the robust optimization technique [21].

In power systems, uncertainty in renewable energy sources and demand can be handled by optimizing base-point generator outputs to meet demand and renewable energy forecasts, whilst satisfying constraints that ensure normal system operation irrespective of the actual demand and output of renewable energy generators. Variations from renewable energy and demand forecasts are then handled by using participation factors to adjust these generator outputs. This participation factor method is explored in [22] and extended in [20]. The main contribution of this work is the extension of this practice to prosumer microgrids with DGs, a battery and dispatchable loads. In the proposed model, DG's, a battery and interruptible loads are assigned participation factors and used to provide robustness against uncertainty in prosumer generation. By involving these grid components, the grid operator has more grid-balancing resources from both the utility and the customer sides of the grid. Moreover, the model could be further advanced, to take advantage of the varying response times of the grid components involved.

The rest of the paper is structured as follows: a brief description of the MG architecture is given in Section 4, and the deterministic and robust optimization models are developed in Section 5. Section 6 contains the MG data and simulation parameters used. Simulation results are presented and discussed in Section 7. A brief conclusion and possible future work are given in Section 8.

4 MG architecture

Figure 1 shows the architecture of an islanded prosumer MG which interconnects DG's, large prosumers, a battery bank, and interruptible and non-interruptible loads. Controllable resources like DG's, the battery and interruptible loads are connected, via local controllers, to a microgrid central controller (MGCC) which is managed by a MGO.

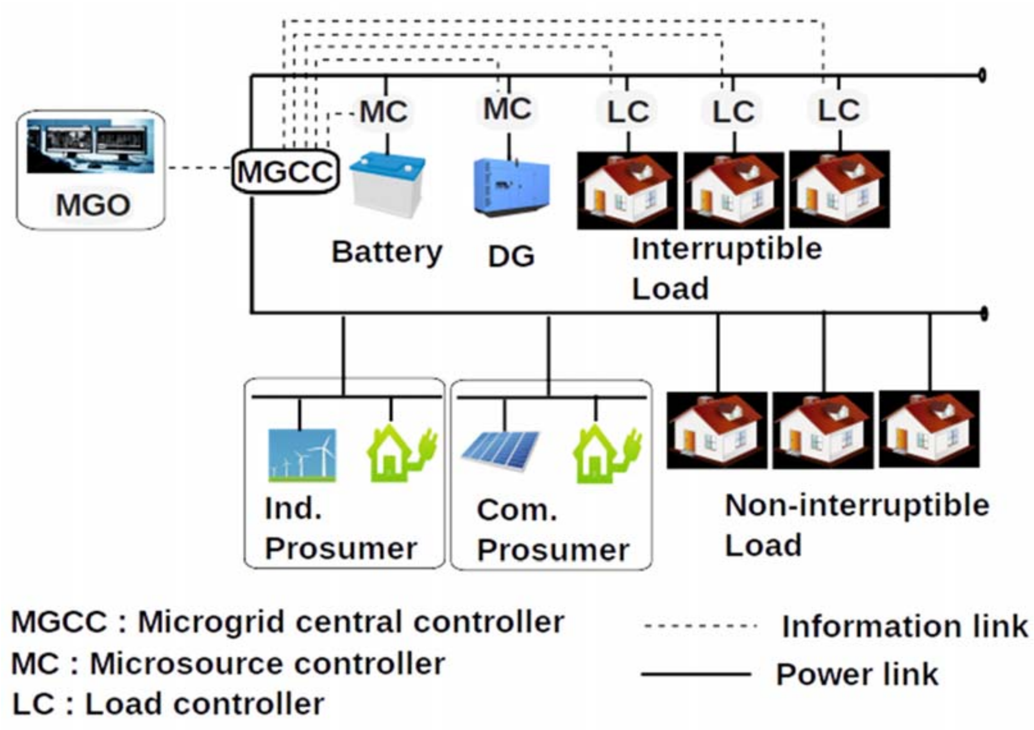

Figure 1 Prosumer MG architecture of a network comprising DG's, a battery, two prosumers, interruptible and uninterruptible loads

5 Mathematical model

5.1 Deterministic model

The MGO's cost metric comprises cost of energy, reserve and up & down regulation from DG's, cost of demand curtailment and cost associated with battery charging and discharging, as detailed in (1).

$$\text{Min} \quad \sum_{g=1}^{G}\left(a_g * \left(P_g^{sch}\right)^2 * \Delta t + b_g * P_g^{sch} * \Delta t\right) + \sum_{g=1}^{G} c * \left(a_g\left(P_g^{res}\right)^2 * \Delta t + b_g * P_g^{res} * \Delta t\right) + \sum_{g=1}^{G} d_g * \left(P_g^{UReg} + P_g^{DReg}\right) + e * P_{curt}^{sch} + f * \left(P_{bToFro}^{sch}\right)^2 \quad (1)$$

In (1), a_g, b_g are cost coefficients of diesel generator g, c_g is the reserve cost factor for diesel generator g, d_g is the cost per unit of up & down regulation of diesel generator g, e is the cost per unit of load curtailed and f is the battery charging/discharging cost factor.

Constraint (2) is enforced to ensure that the resulting scheduled power output and down regulation do not go below the specified minimum power output of DG's.

$$P_g^{min} \leq P_g^{sch} - P_g^{DReg} \quad \forall \mathrm{g} \in [1, \mathrm{G}] \quad (2)$$

Constraints (3) and (4) ensure that the scheduled down & up regulation reserves do not exceed the DG's capability.

$$P_g^{DReg} \leq R_g^D \quad \forall \mathrm{g} \in [1, \mathrm{G}] \quad (3)$$

$$P_g^{UReg} \leq R_g^U \quad \forall \mathrm{g} \in [1, \mathrm{G}] \quad (4)$$

Constraint (5) makes sure that the sum of scheduled energy, reserve and up regulation does not exceed the DG's maximum power output level.

$$P_g^{sch} + P_g^{res} + P_g^{UReg} \leq P_g^{max} \quad \forall \mathrm{g} \in [1, \mathrm{G}] \quad (5)$$

Provision of the required reserve, down regulation and up regulation capacities is guaranteed by enforcing constraints (6), (7) and (8) respectively.

$$\sum_{g=1}^{G} P_g^{res} \geq Res \quad \forall \mathrm{g} \in [1, \mathrm{G}] \quad (6)$$

$$\sum_{g=1}^{G} P_g^{DReg} \geq DReg \quad \forall \mathrm{g} \in [1, \mathrm{G}] \quad (7)$$

$$\sum_{g=1}^{G} P_g^{UReg} \geq UReg \quad \forall \mathrm{g} \in [1, \mathrm{G}] \quad (8)$$

Constraints (9) and (10) ensure that the difference between current power output and scheduled power output of DG does not exceed the DG's regulation limit.

$$P_g^{curr} - P_g^{sch} \leq R_g^D \quad \forall \mathrm{g} \in [1, \mathrm{G}] \quad (9)$$

$$P_g^{sch} - P_g^{curr} \leq R_g^U \quad \forall \mathrm{g} \in [1, \mathrm{G}] \quad (10)$$

Scheduled demand curtailment is kept below (or equal to) the available interruptible load capacity using constraint (11).

$$P_{curt}^{sch} \leq P_{curt}^{max} \quad (11)$$

The rate of charge/discharge is kept within the battery's power capacity using (12). Note that P_{bToFro}^{sch} is positive when the battery is charging, and negative when it is discharging.

$$-P_{bToFro}^{max} \leq P_{bToFro}^{sch} \leq P_{bToFro}^{max} \quad (12)$$

Constraint (13) ensures that the capacity limit of the battery is not exceeded.

$$E_b^{min} \leq E_b + P_{bToFro}^{sch} * \Delta t \leq E_b^{max} \quad (13)$$

Constraints (14) and (15) serve to enforce power balance within prosumers' premises and the MG respectively.

$$P_{proGen,p}^{FC} - P_{proDem,p} + P_{ToFroPro,p} = 0 \quad \forall \mathrm{p} \in [1, \mathrm{P}] \quad (14)$$

$$\sum_{g=1}^{G} P_g^{sch} + P_{curt}^{sch} - P_{bToFro}^{sch} - \sum_{p=1}^{P} P_{ToFroPro,p} - P_D = 0 \tag{15}$$

5.2 Robust model

In this work, prosumer generation forecast error is depicted as $eP_{proGen,p}$, and is within the range $[eP_{proGen,p}^{min}, eP_{proGen,p}^{max}]$. Its determination follows the convention used in [7]. If Γ is taken to be the sum of forecast errors of prosumer generation forecasts then,

$$\Gamma = \sum_{p=1}^{P} eP_{proGen,p} \tag{16}$$

The maximum and minimum values of Γ are therefore expressed respectively in (17).

$$\Gamma^{max} = \sum_{p=1}^{P} eP_{proGen,p}^{max} \ \& \ \Gamma^{min} = \sum_{p=1}^{P} eP_{proGen,p}^{min} \tag{17}$$

The robust formulation generates an optimal base point schedule for DG generation (P_g^{sch}), battery energy transfer (P_{bToFro}^{sch}) and load curtailment (P_{curt}^{sch}). Each DG is assigned a participation factor, λ_g, as well as the battery, λ_b, and demand curtailment, λ_c. After realization of uncertainty, the base point schedules of these components are adjusted by their respective participation factors as shown in (18), (19) & (20).

$$P_g^{act} = P_g^{sch} - \lambda_g \Gamma \qquad \forall g \in [1, G] \tag{18}$$

$$P_{curt}^{act} = P_{curt}^{sch} - \lambda_c \Gamma \tag{19}$$

$$P_{bToFro}^{act} = P_{bToFro}^{sch} + \lambda_b \Gamma \tag{20}$$

λ_g, λ_c & λ_b are non-negative variables.

Inserting (14) into (15), equation (21) is obtained.

$$\sum_{g=1}^{G} P_g^{sch} + P_{curt}^{sch} - P_{bToFro}^{sch} - \sum_{p=1}^{P} \left(P_{proDem,p} - P_{proGen,p}^{FC}\right) - P_D = 0 \tag{21}$$

Upon realization of uncertainty, (21) becomes (22).

$$\sum_{g=1}^{G} P_g^{act} + P_{curt}^{act} - P_{bToFro}^{act} - \sum_{p=1}^{P} \left(P_{proDem,p} - \left(P_{proGen,p}^{FC} + eP_{proGen,p}\right)\right) - P_D = 0 \tag{22}$$

Inserting equations (18) through (20) into (22), (23) is obtained.

$$\sum_{g=1}^{G} \left(P_g^{sch} - \lambda_g \Gamma\right) + P_{curt}^{sch} - \lambda_c \Gamma - \left(P_{bToFro}^{sch} + \lambda_b \Gamma\right) - \sum_{p=1}^{P} \left(P_{proDem,p} - \left(P_{proGen,p}^{FC} + eP_{proGen,p}\right)\right) - P_D = 0 \tag{23}$$

Re-arranging (23), (24) is obtained.

$$\sum_{g=1}^{G} P_g^{sch} + P_{curt}^{sch} - P_{bToFro}^{sch} - \sum_{p=1}^{P} \left(P_{proDem,p} - P_{proGen,p}^{FC}\right) - P_D - \sum_{g=1}^{G} \lambda_g \Gamma - \lambda_c \Gamma - \lambda_b \Gamma + \sum_{p=1}^{P} eP_{proGen,p} = 0 \tag{24}$$

Equation (25) is obtained by inserting (16) into (24).

$$\sum_{g=1}^{G} P_g^{sch} + P_{curt}^{sch} - P_{bToFro}^{sch} - \sum_{p=1}^{P}\left(P_{proDem,p} - P_{proGen,p}^{FC}\right) - P_D - \sum_{g=1}^{G} \lambda_g \Gamma - \lambda_c \Gamma - \lambda_b \Gamma + \Gamma = 0 \qquad (25)$$

Equation (26) is obtained by inserting (21) into (25).

$$\left(1 - \sum_{g=1}^{G} \lambda_g - \lambda_c - \lambda_b\right)\Gamma = 0 \qquad (26)$$

$$\sum_{g=1}^{G} \lambda_g + \lambda_c + \lambda_b = 1 \qquad (27)$$

Equation (27) must be true to ensure energy balance in the MG after realization of uncertainty.

After realization of uncertainty, the inequality in (28) must be enforced for all DG's.

$$P_g^{sch} - P_g^{DReg} \leq P_g^{act} \leq P_g^{sch} + P_g^{UReg} \quad \forall \mathrm{g} \in [1, \mathrm{G}] \qquad (28)$$

Inserting (18) into (28), we get (29).

$$P_g^{sch} - P_g^{DReg} \leq P_g^{sch} - \lambda_g \Gamma \leq P_g^{sch} + P_g^{UReg} \quad \forall \mathrm{g} \in [1, \mathrm{G}] \qquad (29)$$

Re-arranging (29) gives (30).

$$-P_g^{UReg} \leq \lambda_g \Gamma \leq P_g^{DReg} \qquad \forall \mathrm{g} \in [1, \mathrm{G}] \qquad (30)$$

To ensure a feasible DG output for any realization of uncertainty, (30) must hold for any value of Γ.

After realization of uncertainty, (31) must also be enforced for demand curtailment.

$$P_{curt}^{act} \leq P_{curt}^{max} \qquad (31)$$

Inserting (19) into (31), we get (32).

$$0 \leq P_{curt}^{sch} - \lambda_c \Gamma \leq P_{curt}^{max} \qquad (32)$$

To ensure a feasible amount of demand curtailment for any realization of uncertainty, (32) must hold for any value of Γ. After realization of uncertainty, (33) must be enforced for battery power transfer.

$$-P_{bToFro}^{max} \leq P_{bToFro}^{act} \leq P_{bToFro}^{max} \qquad (33)$$

Inserting (20) into (33), we get (34).

$$-P_{bToFro}^{max} \leq P_{bToFro}^{sch} + \lambda_b \Gamma \leq P_{bToFro}^{max} \qquad (34)$$

To ensure a feasible amount of battery power transfer for any realization of uncertainty, (34) must hold for any value of Γ.

After realization of uncertainty, (35) must be enforced for battery capacity.

$$E_b^{min} \leq E_b + P_{bToFro}^{act} * \Delta t \leq E_b^{max} \qquad (35)$$

Inserting (20) into (35), we get (36).

$$E_b^{min} - E_b \leq \left(P_{bToFro}^{sch} + \lambda_b \Gamma\right) * \Delta t \leq E_b^{max} - E_b \qquad (36)$$

To ensure a feasible amount of battery power transfer for any realization of uncertainty, (36) must hold for any value of Γ.

The complete robust formulation is made up of (1) through (10), (14), (15), (27), (30), (32), (34) & (36). Constraints (30), (32), (34) & (36) make the formulation quite difficult to solve as they must be satisfied for all possible realizations of uncertainty. They are therefore simplified as follows:

Constraint (30) would only hold for any value of Γ, if (37) is enforced.

$$\begin{cases} \max\limits_{\Gamma^{min} \le \Gamma \le \Gamma^{max}} \lambda_g \Gamma \le P_g^{DReg} \\ \min\limits_{\Gamma^{min} \le \Gamma \le \Gamma^{max}} \lambda_g \Gamma \ge -P_g^{UReg} \end{cases} \quad \forall g \in [1, G] \tag{37}$$

Similarly, Constraint (32) would only hold for any value of Γ, if (38) is enforced.

$$\begin{cases} \max\limits_{\Gamma^{min} \le \Gamma \le \Gamma^{max}} \lambda_c \Gamma \le P_{curt}^{sch} \\ \min\limits_{\Gamma^{min} \le \Gamma \le \Gamma^{max}} \lambda_c \Gamma \ge P_{curt}^{sch} - P_{curt}^{max} \end{cases} \tag{38}$$

Constraint (34) would only hold for any value of Γ, if (39) is enforced.

$$\begin{cases} \max\limits_{\Gamma^{min} \le \Gamma \le \Gamma^{max}} \lambda_b \Gamma \le P_{bToFro}^{max} - P_{bToFro}^{sch} \\ \min\limits_{\Gamma^{min} \le \Gamma \le \Gamma^{max}} \lambda_b \Gamma \ge -P_{bToFro}^{max} - P_{bToFro}^{sch} \end{cases} \tag{39}$$

Constraint (36) would only hold for any value of Γ, if (40) is enforced.

$$\begin{cases} \max\limits_{\Gamma^{min} \le \Gamma \le \Gamma^{max}} \lambda_b \Gamma \le \frac{E_b^{max} - E_b}{\Delta t} - P_{bToFro}^{sch} \\ \min\limits_{\Gamma^{min} \le \Gamma \le \Gamma^{max}} \lambda_b \Gamma \ge \frac{E_b^{min} - E_b}{\Delta t} - P_{bToFro}^{sch} \end{cases} \tag{40}$$

The inequality constraints (37) through (40) have a form similar to (41), and according to [19], (41) is equivalent to (42). Also, (42) can be transformed into (43) according to [12] hence, (37), (38), (39) and (40) can be replaced with (44), (45), (46) and (47) respectively in the robust model.

$$\begin{cases} \max\limits_{\Gamma^{min} \le \Gamma \le \Gamma^{max}} f(\lambda) \Gamma \le a \\ \min\limits_{\Gamma^{min} \le \Gamma \le \Gamma^{max}} f(\lambda) \Gamma \ge b \end{cases} \tag{41}$$

$$\begin{cases} max(f(\lambda), 0)\Gamma^{max} + min(f(\lambda), 0)\Gamma^{min} \le a \\ max(f(\lambda), 0)\Gamma^{min} + min(f(\lambda), 0)\Gamma^{max} \ge b \end{cases} \tag{42}$$

$$\begin{cases} x_1 \Gamma^{max} + x_2 \Gamma^{min} \le a \\ x_1 \Gamma^{min} + x_2 \Gamma^{max} \ge b \\ x_1 \ge 0; x_1 \ge f(\lambda); x_2 \le 0; x_2 \le f(\lambda) \end{cases} \tag{43}$$

$$\begin{cases} x_1^g \Gamma^{max} + x_2^g \Gamma^{min} \leq P_g^{DReg} \\ x_1^g \Gamma^{min} + x_2^g \Gamma^{max} \geq -P_g^{UReg} \quad \forall g \in [1,G] \\ x_1^g \geq 0; x_1^g \geq \lambda_g; x_2^g \leq 0; x_2^g \leq \lambda_g \end{cases} \tag{44}$$

$$\begin{cases} y_1 \Gamma^{max} + y_2 \Gamma^{min} \leq P_{curt}^{sch} \\ y_1 \Gamma^{min} + y_2 \Gamma^{max} \geq P_{curt}^{sch} - P_{curt}^{max} \\ y_1 \geq 0; y_1 \geq \lambda_c; y_2 \leq 0; y_2 \leq \lambda_c \end{cases} \tag{45}$$

$$\begin{cases} a_1 \Gamma^{max} + a_2 \Gamma^{min} \leq P_{bToFro}^{max} - P_{bToFro}^{sch} \\ a_1 \Gamma^{min} + a_2 \Gamma^{max} \geq -P_{bToFro}^{max} - P_{bToFro}^{sch} \\ a_1 \geq 0; a_1 \geq \lambda_b; a_2 \leq 0; a_2 \leq \lambda_b \end{cases} \tag{46}$$

$$\begin{cases} c_1 \Gamma^{max} + c_2 \Gamma^{min} \leq \frac{E_b^{max} - E_b}{\Delta t} - P_{bToFro}^{sch} \\ c_1 \Gamma^{min} + c_2 \Gamma^{max} \geq \frac{E_b^{min} - E_b}{\Delta t} - P_{bToFro}^{sch} \\ c_1 \geq 0; c_1 \geq \lambda_b; c_2 \leq 0; c_2 \leq \lambda_b \end{cases} \tag{47}$$

The inequality constraints (30), (32), (34) and (36) can now be replaced by (44) through (47); hence, the complete robust formulation is made up of (1) through (10), (14), (15), (27) and (44) through (47).

6 Simulation setup

An MG in Guangdong Province, China is modified and investigated in this study, albeit its power distribution network and associated power flows are not taken into consideration. The MG interconnects 7 similar DG's, an industrial prosumer with wind turbines, a commercial prosumer with solar panels, and a battery storage system. DG parameters are chosen to be a_g= 0.83 \$/(MW^{2}h), b_g=70 \$/MWh, c = 0.5, d = 2.9 \$/MW, $R_g^U = R_g^D$ = 0.025 MW, P_g^{min} = 0, P_g^{max} = 1 MW [22] and P_g^{curr} = 0.7MW. Optimal schedules are expected to be generated every 5 minutes hence Δt = 0.083 hrs. Battery parameters are chosen to be E_b^{min} = 0.1 MWH, E_b^{max} = 3 MWH, E_b = 1.5 MWH and P_{bToFro}^{max}= 0.5 MW. Industrial prosumer (having wind turbines) and commercial prosumer (having solar panels) generation are forecasted to be 2 MW and 0.6 MW respectively with forecast errors of 20 and 10% [7] respectively; their demands are taken to be 0.8 MW and 0.2 MW respectively. The load curtailment cost is taken to be e = 11.81 \$/MW and the cost factor associated with battery charging/discharging is assumed to be f = 1 \$/MW^2. Some other parameters are UReg = Dreg = 0.1 MW, Res = 0.2 MW, P_D= 6.8 MW and P_{curt}^{max} = 1.5 MW. Other data for the MG can be found in [22]. A solver in Advanced Interactive Multidimensional Modelling Systems (which is also used in [23] and [24]) known as CPLEX 12.6.3 (also used in [25]) is used to solve the proposed robust formulation on a PC with processor: Intel(R) Pentium (R) Dual CPU T2390 @ 1.86GHz 1.87 GHz.

7 Discussion of results

Table 1 shows the optimal schedules obtained by both the deterministic and robust formulations. The effect of prosumer generation uncertainty gap, $\Gamma^{max} - \Gamma^{min}$, on the optimal objective value is depicted in Figure 2. Figure 3 is a plot of results obtained by keeping Γ^{max} constant and varying Γ^{min}, and Figure 4 is obtained by keeping Γ^{min} constant and varying Γ^{max}. The robust optimal schedule, as the uncertainty gap is varied, is plotted in Figure 5. Figures 6 & 7 show the optimal schedules generated with respect to magnitude of Γ^{min} and Γ^{max} respectively.

In Table 1, the robust model is seen to yield a higher optimal objective value than the deterministic model; however, it guarantees stable grid operation for any realization of prosumer generation. Note that the DG's, battery and interruptible loads are all used to provide robustness against uncertainty in prosumer generation. Taking a closer look at Table 1, it would be noticed that in seeking a robust solution, the robust formulation sacrifices costs associated with DG generation and demand curtailment, that is, DG output is higher and more demand is curtailed. On the other hand, the discharge rate of the battery is lower for the robust solution. By increasing DG output and demand curtailment, the robust solution protects against scenarios where the actual prosumer generation exceeds the forecasted value (in which case DG output and demand curtailment can be reduced to maintain power balance in the MG). Similarly, by reducing battery discharge rate, the robust solution protects against scenarios where the actual prosumer generation is below the forecasted value (in which case energy deficit can be supplied by the battery to maintain power balance).

Table 1 Optimal schedules by deterministic and robust formulations

Formulation	DG Output (MW)	Battery Power Transfer (MW)	Demand Curtailment (MW)	Optimal Objective value ($)

Deterministic	4.725	-0.475	1E-6	29.059
Robust	5.075	-0.105	0.02	31.467

Note that when uncertainty range is 0 MW, that is, $\Gamma^{max} - \Gamma^{min} = 0$, the robust model generates an optimal schedule equal to that of the deterministic model. Consequently, in Figure 2, the optimal objective value obtained when uncertainty range is 0 MW is equal to that obtained by the deterministic model (shown in Table 1). Notice from Figure 2 that the optimal objective value remains unchanged when uncertainty range increases from 0 MW to 0.2 MW. This suggests that the robust schedule generated for an uncertainty range of 0 MW is able to handle an uncertainty gap of 0.2 MW. For a gap equal to or greater than 0.4 MW, the optimal objective value increases as seen in Figure 2. It is noteworthy to mention that for gaps of 2.4 MW and above, the robust model is infeasible. This is partly due to the physical limitation of DG's (regulation capacity limit) and the battery (power transfer capacity limit).

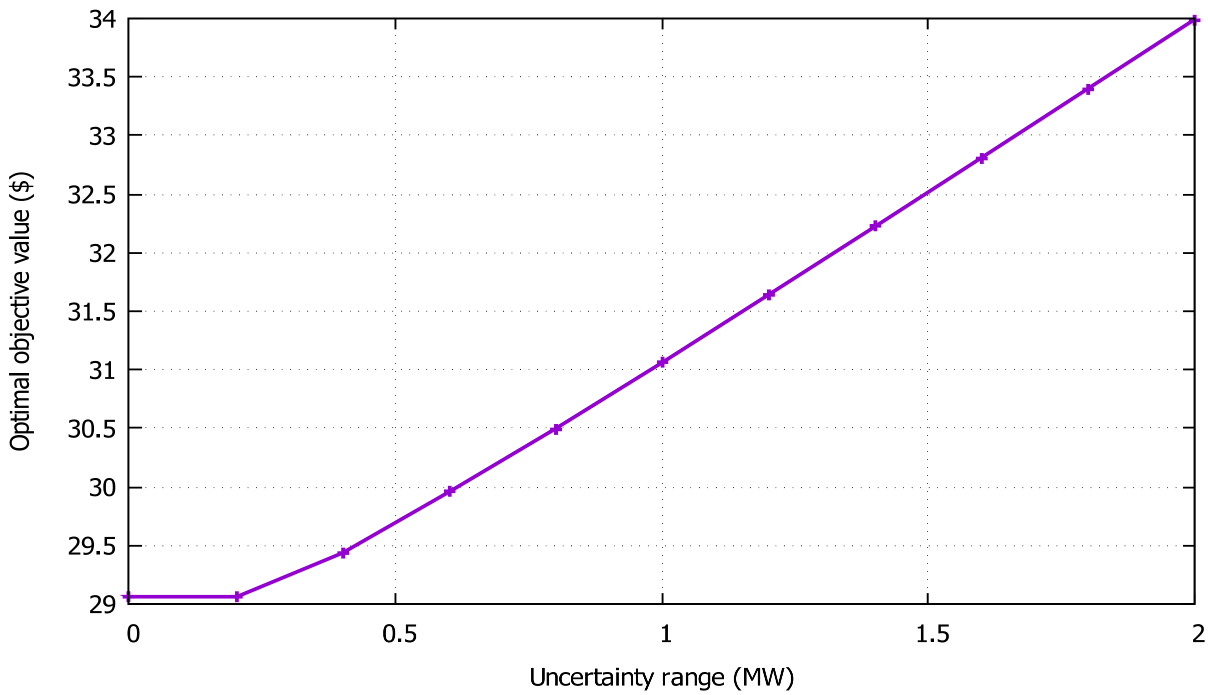

Figure 2 Effect of uncertainty level ($\Gamma^{max} - \Gamma^{min}$) of prosumer generation forecast on the optimal objective value

The plot in Figure 3 is obtained by holding Γ^{max}constant, and varying Γ^{min} from 0 to -2 MW, in steps of – 0.4 MW. The optimal objective value generated at each step is plotted against the magnitude of Γ^{min}. Note that an increase in Γ^{min} increases the uncertainty gap to the left side (lower side) of the forecast.

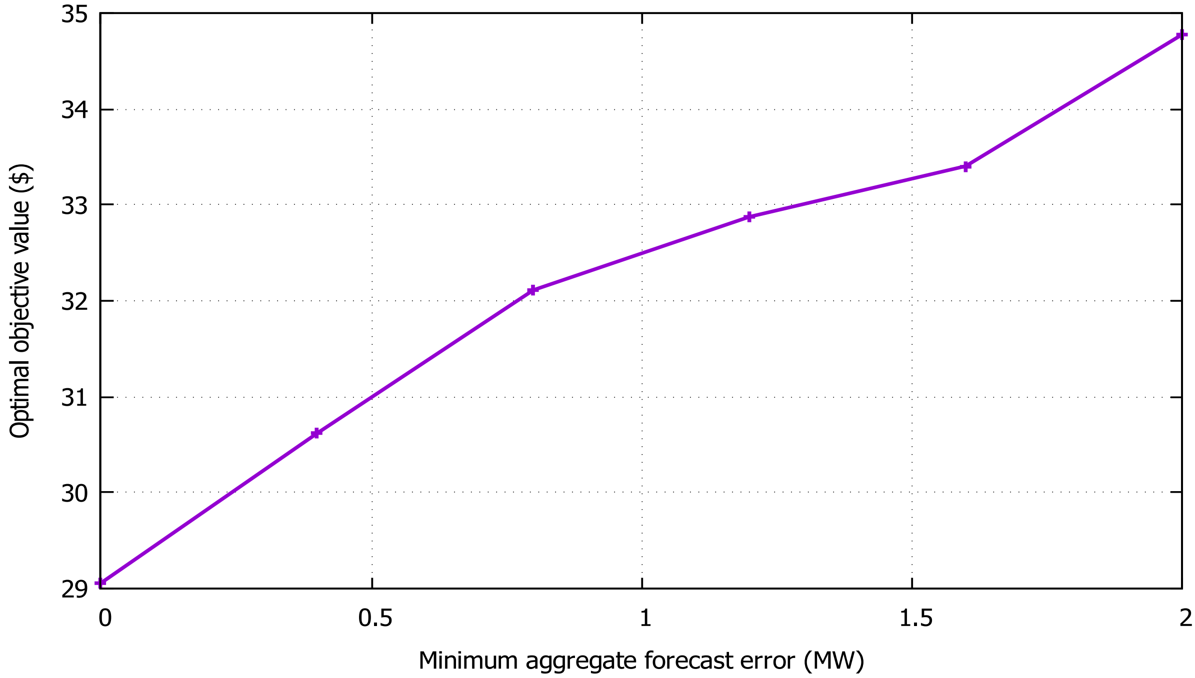

Figure 3 Effect of the magnitude of Γ^{min}(uncertainty gap below the forecast) on the optimal objective value

The plot in Figure 4 is obtained by keeping Γ^{min} constant and varying Γ^{max}. Note again that an increase in Γ^{max} increases the uncertainty gap to the right side (higher side) of the forecast. Similar to the observation made in Figure 2, in Figures 3 & 4, the optimal objective value is seen to increase as the gap widens on either side of the forecast. In addition, it is interesting to note that the maximum value on the "Minimum aggregate forecast error" axis in Figure 3 is 2 MW while that on the "Maximum aggregate forecast error" axis in Figure 4 is 1 MW. This is so because for subsequent values on the axes (2.4 and 1.2 MW respectively), the robust model is infeasible. Hence, the model accommodates a wider uncertainty gap on the left side of the forecast than it does on its right side. This implies that with the state (power output of DG's and energy content of battery) of the MG's components used in the simulation, and component capacity limitations

(DG regulation capacity and battery transfer capacity), the MG is capable of supplying more energy than it can absorb.

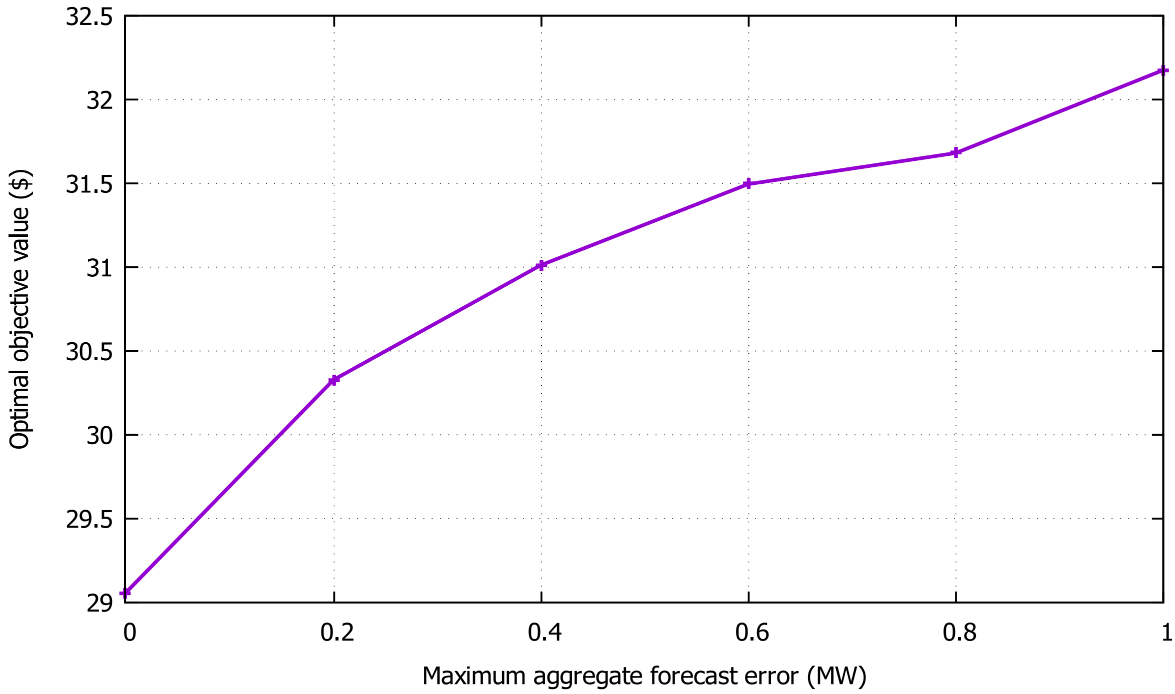

Figure 4 Effect of the magnitude of Γ^{max} (uncertainty gap above the forecast) on the optimal objective value

In Figures 5, 6 & 7, due to the relatively high cost of demand curtailment, the robust solution is reluctant to curtail demand. Also, to maintain power balance, DG schedules can be seen (in Figures 5, 6 & 7) to follow, closely, the trend of battery discharge, that is, as DG output increases, the power from the battery reduces (note that P_{bToFro}^{sch} is positive when the battery is charging, and negative when it is discharging).

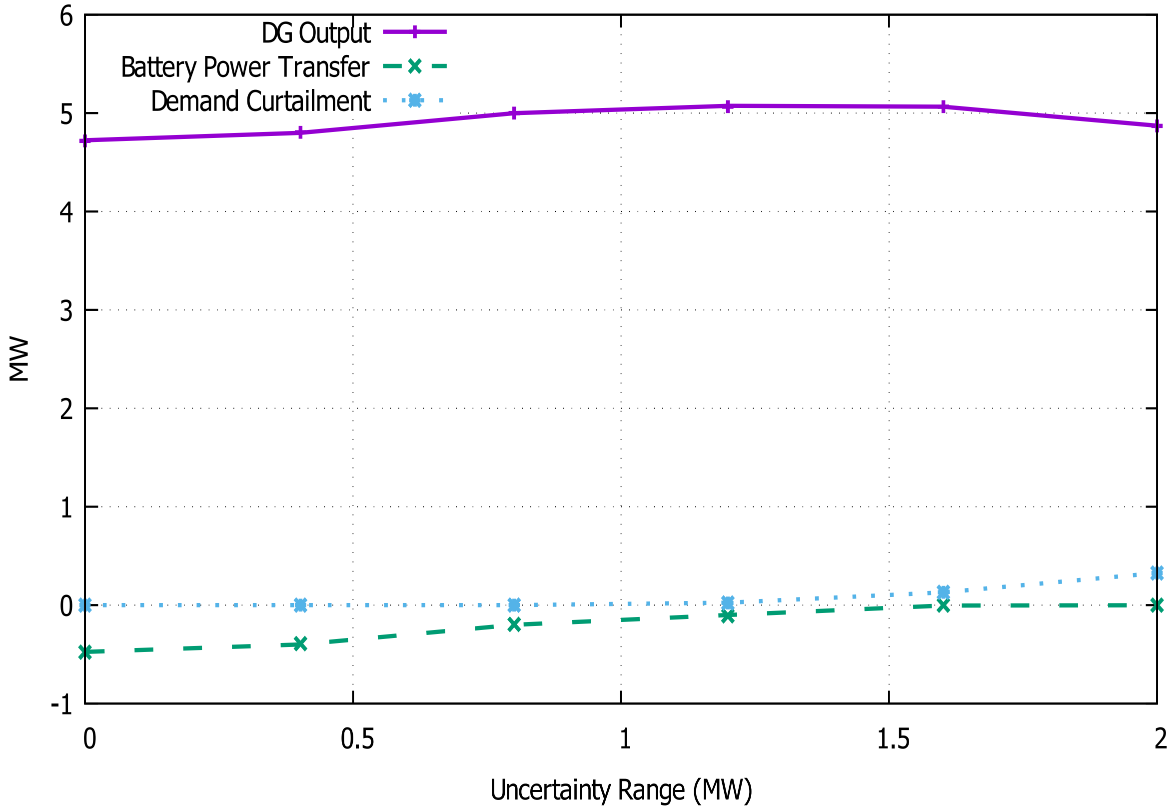

Figure 5 Optimal schedules with respect to uncertainty gap ($\Gamma^{max} - \Gamma^{min}$) in prosumer generation forecast

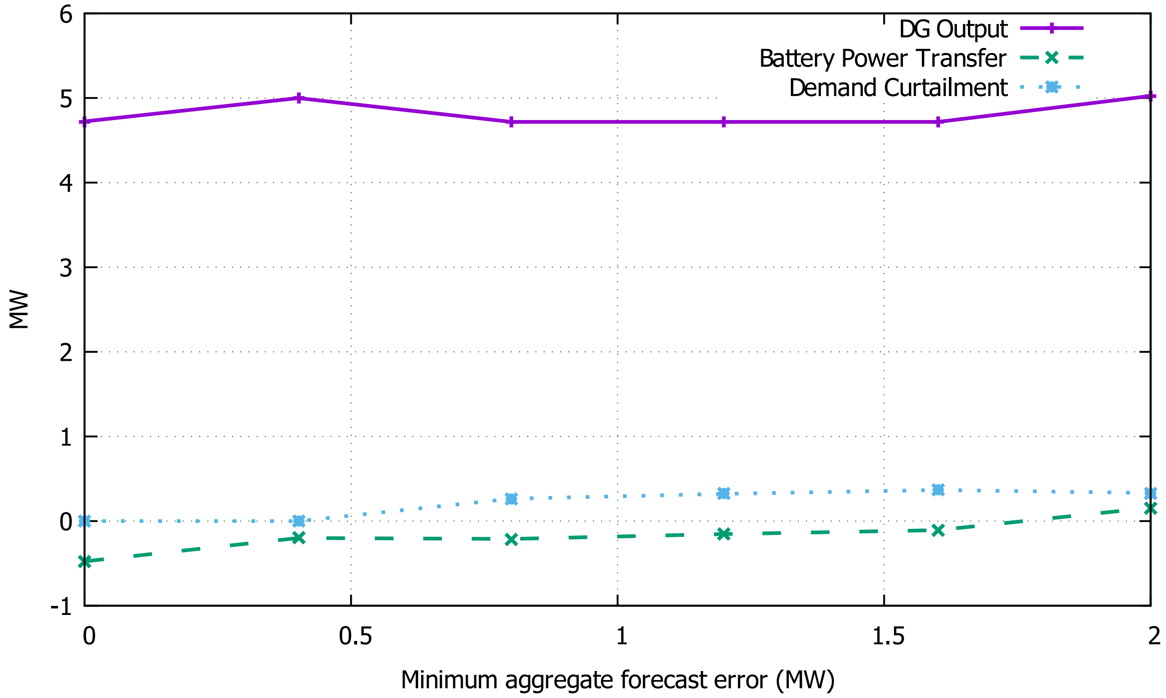

Figure 6 Optimal schedules with respect to magnitude of Γ^{min} (uncertainty gap below the forecast)

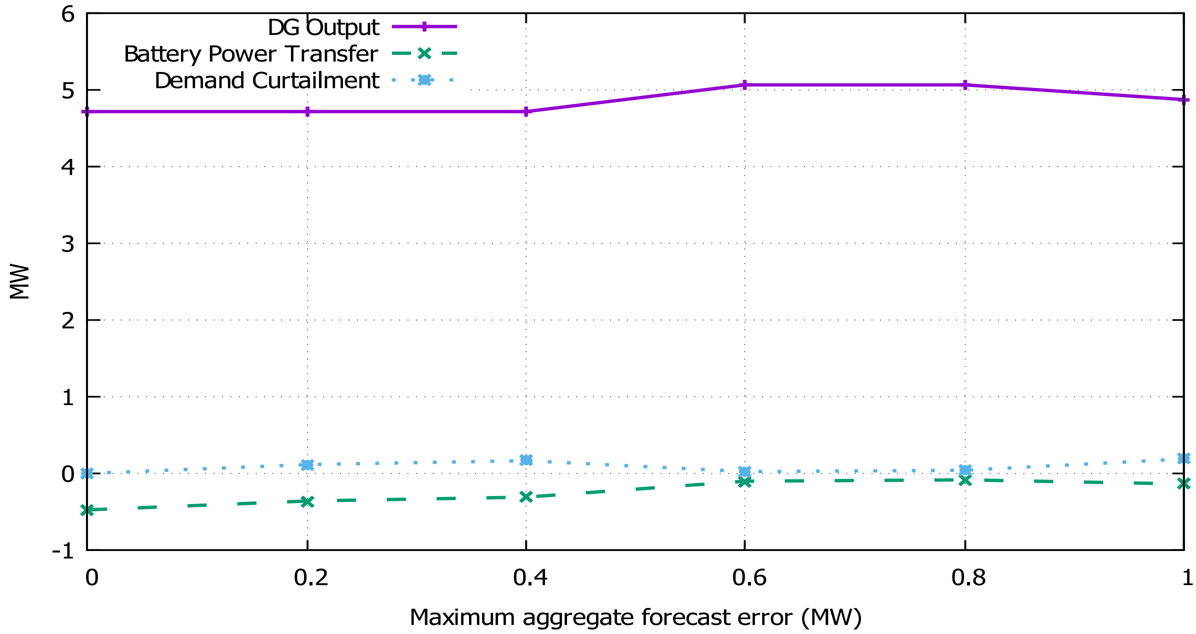

Figure 7 Optimal schedules with respect to magnitude of Γ^{max} (uncertainty gap above the forecast)

In developing a robust energy management model, the authors of [12] assigned participation factors to conventional generators, thereby employing these generators to handle uncertainty in wind power generation. In [20], participation factors were assigned to demand response aggregators, and a robust energy management model which employs these aggregators to handle uncertainty was developed. In this paper, a robust model where participation factors are assigned to conventional generators, a battery and flexible loads is proposed. By involving these grid components, the grid operator has more grid-balancing resources from both the utility and the customer sides of the grid. Moreover, the model could be further advanced, to take advantage of the varying response times of the grid components involved.

8 Conclusion

Extending the approach of participation factors for conventional generators, a computationally tractable robust MG operational dispatch model which uses DG's, battery and interruptible loads to provide robustness against uncertainty in prosumer generation forecast has been developed. The model was tested on a modified version of a MG in China. To ensure robustness to uncertainty in prosumer generation forecast, DG generation and demand curtailment costs were sacrificed by the robust model. Consequently, the robust model yielded a higher objective function value than its deterministic counterpart; however, it guarantees stable system operation for any realization of prosumer generation within specified uncertainty bounds, which the deterministic model cannot guarantee. Simulation results show that the optimal objective value of the robust model increases with the uncertainty gap of prosumer generation forecast. Also, depending on the status of DG's and battery (that is, power output of DG's and energy content of battery), and their capacity limitations (that is, DG regulation capacity and battery transfer capacity), an MG may capable of supplying more energy than it can absorb.

This work may be extended by incorporating power flows and system constraints associated with the underlying MG distribution network into the robust model.

References

[1] Zafar, R., Mahmood, A., Razzaq, S., Ali, W., Naeem, U. and Shehzad, K., 2017. Prosumer based energy management and sharing in smart grid. *Renewable and Sustainable Energy Reviews*.

[2] Wang, J., Redondo, N.E. and Galiana, F.D., 2003. Demand-side reserve offers in joint energy/reserve electricity markets. *IEEE Transactions on Power Systems*, *18*(4), pp.1300-1306.

[3] Zakariazadeh, A. and Jadid, S., 2014. Smart microgrid operational planning considering multiple demand response programs. *Journal of Renewable and Sustainable Energy*, *6*(1), p.013134.

[4] Zakariazadeh, A., Jadid, S. and Siano, P., 2014. Smart microgrid energy and reserve scheduling with demand response using stochastic optimization. *International Journal of Electrical Power & Energy Systems*, *63*, pp.523-533.

[5] Zakariazadeh, A., Jadid, S. and Siano, P., 2014. Economic-environmental energy and reserve scheduling of smart distribution systems: A multiobjective mathematical programming approach. *Energy Conversion and Management*, *78*, pp.151-164.

[6] Mohan, V., Singh, J.G. and Ongsakul, W., 2015. An efficient two stage stochastic optimal energy and reserve management in a microgrid. *Applied energy*, *160*, pp.28-38.

[7] Damisa, U., Nwulu, N.I. and Sun, Y., 2018. microgrid energy and reserve management incorporating prosumer behind-the-meter resources. *IET Renewable Power Generation*, *12*(8), pp.910-919.

[8] Golshannavaz, S., Afsharnia, S. and Siano, P., 2016. A comprehensive stochastic energy management system in reconfigurable microgrid s. *International Journal of Energy Research*, *40* (11), pp.1518-1531.

[9] Tabar, V.S., Jirdehi, M.A. and Hemmati, R., 2017. Energy management in microgrid based on the multi objective stochastic programming incorporating portable renewable energy resource as demand response option. *Energy*, *118*, pp.827-839.

[10] Hu, M.C., Lu, S.Y. and Chen, Y.H., 2016. Stochastic programming and market equilibrium analysis of microgrid s EM systems. *Energy*, *113*, pp.662-670.

[11] Shen, J., Jiang, C., Liu, Y. and Wang, X., 2016. A Microgrid Energy Management System and Risk Management Under an Electricity Market Environment. *IEEE Access*, *4*, pp.2349-2356.

[12] Ding, T., Wu, Z., Lv, J., Bie, Z. and Zhang, X., 2016. Robust co-optimization to energy and ancillary service joint dispatch considering wind power uncertainties in real-time electricity markets. *IEEE Transactions on Sustainable Energy*, *7*(4), pp.1547-1557.

[13] Liu, J., Chen, H., Zhang, W., Yurkovich, B. and Rizzoni, G., 2017. Energy Management problems under uncertainties for grid-connected microgrids: a chance constrained programming approach. *IEEE Transactions on Smart Grid*, *8*(6), pp.2585-2596.

[14] Ackooij, W.V., Zorgati, R., Henrion, R. and Möller, A., 2011. Chance constrained programming and its applications to energy management, stochastic optimization. *Anonymous InTech*.

[15] Ben-Tal, A., El Ghaoui, L. and Nemirovski, A., 2009. *Robust optimization* (Vol. 28). Princeton University Press.

[16] Xiang, Y., Liu, J. and Liu, Y., 2016. Robust energy management of microgrid with uncertain renewable generation and load. *IEEE Transactions on Smart Grid*, *7*(2), pp.1034-1043.

[17] Hu, W., Wang, P. and Gooi, H.B., 2018. Toward optimal energy management of microgrids via robust two-stage optimization. *IEEE Transactions on Smart Grid*, *9*(2), pp.1161-1174.

[18] Guo, Y. and Zhao, C., 2018. Islanding-aware robust energy management for microgrids. *IEEE Transactions on Smart Grid*, *9*(2), pp.1301-1309.

[19] Jabr, R.A., 2013. Adjustable robust OPF with renewable energy sources. *IEEE Transactions on Power Systems*, *28*(4), pp.4742-4751.

[20] Damisa, U., Nwulu, N.I. and Sun, Y., 2018. A robust energy and reserve dispatch model for prosumer microgrids incorporating demand response aggregators. *Journal of Renewable and Sustainable Energy*, *10*(5), p.055301.

[21] Bertsimas, D. and Sim, M., 2004. The price of robustness. *Operations research*, *52*(1), pp.35-53.

[22] Shi, W., Xie, X., Chu, C.C.P. and Gadh, R., 2015. Distributed Optimal energy management in microgrids. *IEEE Trans. Smart Grid*, *6*(3), pp.1137-1146.

[23] Nwulu, N.I. and Xia, X., 2015. Implementing a model predictive control strategy on the dynamic economic emission dispatch problem with game theory based demand response programs. *Energy*, *91*, pp.404-419.

[24] Nwulu, N.I. and Xia, X., 2015. Multi-objective dynamic economic emission dispatch of electric power generation integrated with game theory based demand response programs. *Energy Conversion and Management*, *89*, pp.963-974.

[25] Gbadamosi, S.L., Nwulu, N.I. and Sun, Y., 2018. Multi-objective optimization for composite generation and transmission expansion planning considering offshore wind power and feed-in tariffs. *IET Renewable Power Generation*, *12*(14), pp.1687-1697.